Targeting PI3K/mTOR signaling exerts potent antitumor activity in pheochromocytoma *in vivo*

Misu Lee[1,*], Ninelia Minaskan[1], Tobias Wiedemann[1], Martin Irmler[2], Johannes Beckers[2,3,4], Behrooz H Yousefi[5], Georgios Kaissis[6], Rickmer Braren[6], Iina Laitinen[7,†] and Natalia S Pellegata[1]

[1]Institute for Diabetes and Cancer, Helmholtz Zentrum München, Neuherberg, Germany
[2]Institute of Experimental Genetics, Helmholtz Zentrum München, Neuherberg, Germany
[3]German Center for Diabetes Research (DZD), Neuherberg, Germany
[4]Technische Universität München, Chair of Experimental Genetics, Freising, Germany
[5]Department of Pharmaceutical Radiochemistry, Technische Universität München, Garching, Germany
[6]Institute for Diagnostic and Interventional Radiology, Klinikum rechts der Isar der Technische Universität München, Munich, Germany
[7]Department of Nuclear Medicine, Klinikum rechts der Isar der Technische Universität München, Munich, Germany
*(M Lee is now at Division of Life Sciences, College of Life Science and Bioengineering, Incheon National University, Incheon, Korea)
†(L Laitinen is now at Sanofi-Aventis Deutschland GmbH, Germany)

Correspondence should be addressed to N S Pellegata
Email
Natalia.pellegata@helmholtz-muenchen.de

Endocrine-Related Cancer

Abstract

Pheochromocytomas (PCCs) are mostly benign tumors, amenable to complete surgical resection. However, 10–17% of cases can become malignant, and once metastasized, there is no curative treatment for this disease. Given the need to identify the effective therapeutic approaches for PCC, we evaluated the antitumor potential of the dual-PI3K/mTOR inhibitor BEZ235 against these tumors. We employed an *in vivo* model of endogenous PCCs (MENX mutant rats), which closely recapitulate the human tumors. Mutant rats with PCCs were treated with 2 doses of BEZ235 (20 and 30 mg/kg), or with placebo, for 2 weeks. Treatment with BEZ235 induced cytostatic and cytotoxic effects on rat PCCs, which could be appreciated by both staining the tumors *ex vivo* with appropriate markers and non-invasively by functional imaging (diffusion-weighted magnetic resonance imaging) *in vivo*. Transcriptomic analyses of tumors from rats treated with BEZ235 or placebo-identified potential mediators of therapy response were performed. *Slc6a2*, encoding the norepinephrine transporter (NET), was downregulated in a dose-dependent manner by BEZ235 in rat PCCs. Moreover, BEZ235 reduced *Slc6a2*/NET expression in PCC cell lines (MPC) also. Studies of a BEZ235-resistant derivative of the MPC cell line confirmed that the reduction of NET expression associates with the response to the drug. Reduction of NET expression after BEZ235 treatment *in vivo* could be monitored by positron emission tomography (PET) using a tracer targeting NET. Altogether, here we demonstrate the efficacy of BEZ235 against PCC *in vivo*, and show that functional imaging can be employed to monitor the response of PCC to PI3K/mTOR inhibition therapy.

Key Words
- pheochromocytoma
- MENX
- PI3K/mTOR inhibition
- NET
- predictive biomarker
- imaging

Endocrine-Related Cancer (2017) **24**, 1–15

http://erc.endocrinology-journals.org
DOI: 10.1530/ERC-16-0324

Published by Bioscientifica Ltd.

Introduction

Pheochromocytomas (PCCs) and paragangliomas (PGLs) are rare neuroendocrine tumors derived from chromaffin cells of the adrenal medulla and paraganglia of the autonomic nervous system, respectively (Lenders *et al.* 2005). The majority of these tumors are benign, amenable to complete surgical resection with a high survival rate for patients. However, 10–17% of the cases (up to 25% depending on the genetic predisposition) can become malignant, and once metastasized, no curative treatment currently exists for this disease (Eisenhofer *et al.* 2004). In inoperable patients, systemic chemotherapy with cyclophosphamide, vincristine and doxorubicin (CVD) was tested, but no statistically significant difference in overall survival was observed between patients whose tumors responded to CVD therapy and those whose tumors did not (Averbuch *et al.* 1988, Huang *et al.* 2008). Radiotherapy with the radiopharmaceutical [^{131}I]-meta-iodobenzylguanidine (MIBG), an analogue of norepinephrine, is the only currently available therapeutic option for patients with unresectable or malignant PCCs or PGLs, and may have positive therapeutic effects, but tumor regression has been seen in only 30% of patients (Loh *et al.* 1997). In a few case reports, the multi-tyrosine kinase inhibitor sunitinib has shown some efficacy in the therapy of patients with progressive disease (Joshua *et al.* 2009). Altogether, despite the clinical need, no effective therapies have been so far developed for patients with aggressive PCC.

PCCs/PGLs occur sporadically or as a result of an inherited germline mutation in one of at least 15 genes (35–40% of cases), including *VHL*, *NF1*, *RET*, *SDHA*, *SDHB*, *SDHC*, *SDHD*, *SDHAF2*, *HIF2α*, *TMEM127*, *MAX* and *FH* (Moraitis *et al.* 2014). Transcriptome analyses have shown that gene expression signatures of human PCCs reflect the underlying driver mutation (Moraitis *et al.* 2014). Specifically, they can be divided into two main clusters: cluster 1 tumors are associated with mutations in genes that ultimately result in the stabilization of hypoxia-inducible factors (HIFs), particularly HIF2α, whereas cluster 2 PCCs bear mutations affecting tyrosine kinase signaling. Cluster 1 human PCCs are more aggressive, develop at both adrenal and extra-adrenal locations, occur at a younger age, do not express phenylethanolamine N-methyltransferase (PNMT), the enzyme that converts noradrenaline to adrenaline, and have an immature catecholamine secretory behavior (Eisenhofer *et al.* 2011).

Activation of the PI3K/AKT/mTOR pathway plays a pivotal role in the initiation and progression of many human malignancies by enhancing cell survival, stimulating cell proliferation and inhibiting apoptosis (Cantrell 2001, Hennessy *et al.* 2005). Constitutive activation of the PI3K/AKT/mTOR signaling cascade is also a feature of PCCs, and it is associated to overexpression of phosphorylated (P)-AKT (Fassnacht *et al.* 2005). Thus, agents inhibiting PI3K signaling might represent an effective therapeutic option for these tumors. So far, the mTOR inhibitor everolimus (RAD001) has been tested in few patients with progressive/malignant PCC, but exhibited a low efficacy (Druce *et al.* 2009, Oh *et al.* 2012). The lack of tumor control in these patients could be due to a feedback loop mechanism, which can re-activate AKT signaling upstream of mTOR, thereby re-stimulating the pathway. This is a well-documented mechanism of resistance to rapamycin and its analogues in various human cancers, which abrogates their initial antitumor effects (Hosoi *et al.* 1998, Porta *et al.* 2014). Along these lines, it has been shown that metastatic PCCs associated with *SDHB* mutations do not express P-mTOR and P-S6 at high levels, thereby suggesting that therapies targeting mTORC1 alone (the rapamycin-sensitive component of mTOR) might not be effective at controlling these aggressive tumors (Ghayee *et al.* 2013). To circumvent these issues, compounds able to inhibit the two components of mTOR (mTORC1 and mTORC2) or both mTOR and the upstream PI3K kinase were generated. The latter group includes BEZ235, a synthetic small molecule, which inhibits both PI3K and mTORC1/2 kinase activity by binding to the ATP-binding cleft of these enzymes (Maira *et al.* 2008). BEZ235 has shown potent anti-proliferative activity in preclinical models of several tumor types (Maira *et al.* 2008, Schnell *et al.* 2008, Serra *et al.* 2008, Baumann *et al.* 2009, Cao *et al.* 2009) and is currently evaluated in Phase I/II clinical trials in patients with advanced solid tumors. It has been shown that BEZ235 displays antitumor effects against PCC cell lines (MPC and MTT) *in vitro* (Nölting *et al.* 2012).

MENX is a multiple endocrine neoplasia syndrome in the rat, which is caused by a homozygous germline mutation in the *Cdkn1b* gene encoding the cell cycle inhibitor p27 (Pellegata *et al.* 2006). MENX-affected rats develop, among other endocrine tumors, bilateral PCCs with complete penetrance at 6–8 months of age. Our previous work has shown that endogenous PCCs developing in MENX-affected rats share similarities with their human counterpart. Specifically, rat PCCs

http://erc.endocrinology-journals.org
DOI: 10.1530/ERC-16-0324

Published by Bioscientifica Ltd.

have histopathological features similar to human PCCs (Shyla *et al.* 2010) and show elevated proliferation rates (average 11.3%) (Miederer *et al.* 2011), thus mostly resembling aggressive human tumors. Rat PCCs do not express PNMT and should be noradrenergic (Molatore *et al.* 2010). Measurements of urine catecholamine levels confirmed this hypothesis. Indeed, when compared to wild-type rats, the mutant animals show age-dependent increases in urinary outputs of norepinephrine and normetanephrine, which correlate in time with the development of tumor nodules, increase in blood pressure and development of hypertension-related end-organ pathology (Wiedemann *et al.* 2016). Moreover, the rat tumors share gene copy number variations (Shyla *et al.* 2010) and gene expression signatures (Molatore *et al.* 2010) with the human tumors. This has been exploited to identify novel molecular mechanisms involved in human PCCs (e.g. the pro-oncogenic role of BMP7) (Leinhäuser *et al.* 2015). Interestingly, given that rat PCCs show upregulation of the *Hif2α* gene, but not of *Hif1α*, can develop at extra-adrenal locations (Molatore *et al.* 2010), do not express PNMT and display a more immature secretory phenotype (Wiedemann *et al.* 2016), they are more similar to cluster 1 human tumors. Noteworthy, the similarities between rat and human PCCs also extend to the uptake of radiolabelled tracers for functional imaging. Indeed, the rat tumors showed uptake of tracers used for PCC diagnosis in the clinics and targeting the norepinephrine transporter (NET) system (e.g. MIBG; hydroxyephedrine-HED) (Miederer *et al.* 2011), the aromatic amino acid transporter and L-amino acid decarboxylase (DOPA) (Pellegata, unpublished) or somatostatin receptors (e.g. ^{68}Ga-DOTATOC) (Miederer *et al.* 2011). Rat PCC could also be well visualized using a novel norepinephrine analogue suitable for positron emission tomography (PET), i.e. LMI1195 (Gaertner *et al.* 2013).

Given that, similar to human PCCs, the rat tumors show hyperactivation of the PI3K/AKT/mTOR pathway, we evaluated the efficacy of BEZ235 against rat primary PCC cells *in vitro* and found that this drug can reduce their viability (–22%) (Lee *et al.* 2012). In the current study, we expanded these studies to include the evaluation of BEZ235 administration to MENX rats, with the aim of verifying the antitumor effect of the drug on PCC *in vivo*. Moreover, we wanted to identify the molecular readouts of drug treatment. We evaluated two doses of BEZ235 *in vivo* and performed functional imaging to confirm the cytotoxic effect of the drug. Genome-wide transcriptome profiling of PCCs from drug-treated or placebo-treated rats was conducted, and identified the *Slc6a2* gene, encoding the NET protein, as a target of BEZ235, which is inhibited by drug treatment. Functional analyses confirmed a predictive role for NET expression in the response to PI3K/mTOR inhibition, which can be monitored using NET-selective functional positron emission tomography (PET) imaging with ^{18}F-LMI1195.

Materials and methods

Animals

MENX-affected Sprague-Dawley rats (hereafter indicated as mutant) were maintained in agreement with general husbandry rules approved by the Helmholtz Zentrum München and by the Technische Universität München. Experiments were conducted with animals between 7 and 8 months of age (with tumors). The experimental protocol was approved by the local government authority for animal research (Regierung von Oberbayern, Munich, Germany).

Compound preparation and *in vivo* treatment

BEZ235 was kindly provided from Novartis Pharma. For *in vitro* studies, stock solutions of BEZ235 was prepared in 100% DMSO and stored at –20°C. Dilutions to the final concentration were made in the culture medium immediately before use. For *in vivo* experiments, BEZ235 was resuspended in 1 volume of 1-methyl-2-pyrrolidone (Sigma-Aldrich) and 9 volumes of PEG300 (Sigma-Aldrich).

Mutant rats were treated for 14 days with BEZ235 (20 or 30 mg/kg) or placebo (PEG) administered daily per oral gavage. These drug concentrations were chosen because they are not associated to significant weight loss. Our primary end points were functional/molecular tumor changes, the secondary end points were tumor size changes.

Cell culture

MPCs were kindly provided by Dr Arthur Tischler (Tufts Medical Center, Boston, MA, USA) and MTT cells by Dr Karel Pacak (NIH) and cultured in DMEM medium (Thermo Fisher Scientific) containing 10% FCS and 100 Units Penicillin/100 µg Streptomycin at 37°C in a 5% CO_2 atmosphere. PC12 cells were purchased from LGC Promochem (European ATCC Distributor). The cell line was cultured in FK12 (DMEM), medium with 15% (v/v)

http://erc.endocrinology-journals.org
DOI: 10.1530/ERC-16-0324

Published by Bioscientifica Ltd.

horse serum, 2.5% (v/v) FBS and 1% (v/v) penicillin–streptomycin. All cells were only passaged *in vitro* for 3–5 passages and then new aliquots were thawed. Cell lines were routinely checked for mycoplasma contamination using the MycoAlert Detection Kit (Lonza Group Ltd, Basel, CH, Switzerland). MPCR cells, a MPC-derived and BEZ235-resistant clonal cell population, were obtained by chronic exposure to BEZ235 for eight weeks. Initially, cells were treated with 1 µM BEZ235 or DMSO (as control) for 72 h. The media was removed, and cells were allowed to recover for a further 72 h. We carried out this process for approximately 8 weeks. Cells were then maintained continuously in the presence of BEZ235 or DMSO.

Primary pheochromocytoma tumor cells from mutant rat were isolated as previously reported (Lee *et al.* 2012). Briefly, the cells were seeded in 96-well plates (25,000 cells per well) and left for 36 h at 37°C in a humidified incubator with 5% CO_2 in air before beginning the treatments.

In vitro assays

To examine their clonogenic activity, MPC and MPCR cells were plated (100,000 per well) in 6-well plates. The next day, the cells were incubated for 6 weeks in medium containing 1 µM BEZ235 or DMSO. The medium was changed every 3 days. They were then stained with 0.3% crystal violet in 30% ethanol.

Caspase-3/7 activity was assessed in MPC and MPCR cells using a proluminescent caspase-3/7 substrate, which contains the tetrapeptide sequence DEVD (Caspase-Glo 3/7 kit, Promega). Luminescence was measured with a luminometer (Tecan Group Ltd, Männedorf, CH, Switzerland).

Migration and invasion assays

Chemomigration assays were performed using 24-well plates with uncoated polycarbonate membrane inserts (BD BioCoat, BD, Heidelberg, Germany). A total of 100,000 MPC cells were added onto the insert. The lower well was filled with a medium complemented with 2.5% FBS and 15% horse serum. Migrated cells were fixed 24 h later in 100% methanol and stained with 1.5% (w/v) crystal violet in water. Invasion assays were performed with matrigel-coated polycarbonate membrane inserts (BD BioCoat, BD) according to the manufacturer's recommendations. We plated 150,000 MPC cells for these assays and 48 h later cells were fixed and stained as indicated previously for migration assays.

Protein extraction and western blotting

For protein extraction, cells were collected after treatments, washed twice in PBS and lysed in lysis buffer essentially as previously reported (Lee *et al.* 2012). Protein concentration was assessed by the bicinchoninic acid assay (Thermo Fisher Scientific). Total extracts were subjected to polyacrylamide gel electrophoresis by using Bis–Tris 4–12% NuPAGE gels, blotted and probed with the following monoclonal antibodies: against NET (clone 05-1; MAb Technologies, Stone Mountain, GA, USA), total AKT (#9272s), phosphorylated (P)-AKT (Ser473) (#4060), total S6 (#2217), P-S6 (Ser240/244) (#2211) all from Cell Signaling Technology, Annexin V (ab14196; Abcam), NuSAP (#12024-1-AP; Proteintech, Chicago, IL, USA) and α-tubulin (Sigma-Aldrich). Immunoreactive proteins were visualized by using West Pico chemiluminescent substrates (Thermo Fisher Scientific).

Immunostainings

Tumor tissues from MENX rats were collected after 2 weeks of treatment with BEZ235 (20 or 30 mg/kg) or placebo (PEG). They were fixed with 4% paraformaldehyde and embedded in paraffin. Immunohistochemistry (IHC) was performed on 2 µM tissue sections using an automated immunostainer (Ventana Medical Systems, Tucson, AZ, USA), as previously described (Molatore *et al.* 2010). The antibody against NET (clone 05-1; 1:350; MAb Technologies) was diluted in Dako REALTM antibody diluent (Dako). The SuperSentitive IHC detection system from BioGenex (Freemont, CA, USA) was used to visualize the antibody binding following the manufacturer's instructions. Images were recorded using a Hitachi camera HW/C20 (Hitachi High-Technologies) installed in a Zeiss Axioplan microscope with Intellicam software (Carl Zeiss MicroImaging).

Immunofluorescence (IF) was conducted on 2 µm tissue sections using established protocols (Lee *et al.* 2015). Primary antibodies for IF were directed against monoclonal phospho (p)-S6 (S6-S240/244; #2211; 1:500; Cell Signaling Technology), monoclonal Ki67 (clone B56, 1:100; Dako), NuSAP (#12024-1-AP, 1:100; Proteintech), CD31 (#ab28364; 1:75; AbCam), VEGF (clone C20, # sc-152; 1:200; Santa Cruz), polyclonal-activated caspase-3 (#9664, 1:100; Cell Signaling) and Annexin V (ab14196; 1:100; Abcam). Secondary antibodies used for IF were anti-mouse Alexa Fluor 555-conjugated antibody (Cell Signaling Technology) or anti-rabbit

http://erc.endocrinology-journals.org
DOI: 10.1530/ERC-16-0324

Published by Bioscientifica Ltd.

FITC-conjugated antibody (Invitrogen) (Leinhäuser *et al.* 2015). Sections were then analyzed with a Zeiss Axiovert 200 epifluorescence microscope including Apotome unit (Carl Zeiss MicroImaging). Quantification of P-S6, CD31, VEGFA, active caspase-3 and Annexin V staining intensity was performed using ImageJ (NIH). Images were subjected to the threshold function, and we used the same threshold for all images obtained with the same antibody. Then, the percentage of the area with positive signal was determined. The Ki67 labeling index (LI = percentage of positive nuclei) was estimated as previously reported (Lee *et al.* 2015).

For immunocytochemistry, 2500 rat primary PCC cells were plated on Thermo Scientific Nunc Lab-Tek II Chamber Slide (Thermo Scientific).

RNA isolation, RT-PCR and microarray preparation

RNA was extracted from cell lines or from macrodissected, frozen rat PCC samples after standard protocols (Molatore *et al.* 2010). For semi-quantitative RT-PCR, 1000 ng of total RNA was reverse-transcribed and amplified using primers specific for the rat or mouse *Slc6a2* genes. The rat or mouse *Gapdh* gene was amplified in parallel to control for RNA amount. Primer sequences are Rat NET_FW 5′-GGTGCCTTCCTGATTCCATA-3′, Rat NET_Rev 5′-GGATCACAGCATAGCCCACT-3′, Mouse NET_FW 5′-CCATACCAAATACTCCAAATACAAG-3′, Mouse NET_Rev 5′-CGTGAAGAGTTTCCGGTGTCGCTT-3′. Only data from the exponential phase of the amplification were used.

Quantitative RT-PCR was performed using single TaqMan inventoried primers and probes (Applied Biosystems) for the indicated genes. Sequence of TaqMan assays are rat *Slc6a2* CAGAGTTTTATGAGCGTGGTGTCC and mouse *Slc6a2* TGCGGAGTTTTATGAACGCGGAGTC.

For microarray analysis, total RNA (30 ng) was amplified using the Ovation PicoSL WTA System V2 in combination with the Encore Biotin Module (Nugen, Leek, The Netherlands). Amplified cDNA was hybridized on Affymetrix Rat Gene 1.0 ST arrays (Affymetrix). Staining and scanning was done according to the Affymetrix expression protocol including minor modifications as suggested in the Encore Biotin protocol.

Biostatistical and bioinformatic analysis

Expression console (Affymetrix) was used for quality control and to obtain annotated normalized RMA (Robust Multi-Array Average) gene-level data (standard settings including median polish and sketch-quantile normalization). Statistical analysis was done in TM4 (Saeed *et al.* 2003), and heat maps were generated in CARMAweb (Rainer *et al.* 2006). Genewise testing for differential expression was done using two-factor ANOVA and Benjamini–Hochberg multiple testing correction (FDR < 10%). Also, the *P* value of the ANOVA was used to define sets of regulated genes ($P < 0.01$). The pathway analyses were generated through the use of QIAGEN's Ingenuity Pathway Analysis (IPA, QIAGEN Redwood City, www.qiagen.com/ingenuity). Array data were submitted to Gene Expression Omnibus (GSE83401).

Magnetic resonance imaging (MRI)

MRI was performed using a 3.0-T clinical MRI system (Ingenia 3.0 T; Philips Healthcare) prior and 2 weeks after treatment with BEZ235 essentially as reported (Lee *et al.* 2015). Anesthetized animals (2.5% isoflurane, administered in pure oxygen) were placed in a standard human wrist coil (SENSE Wrist coil 8 elements; Philips Healthcare) in a prone position. T2-weighted (T2w) turbo spin echo sequence (slice thickness = 0.7 mm, in plane resolution $0.3 \times 0.3\,mm^2$, TR/TE = 3399/106 ms, averages = 12) was performed to assess the tumor volume before and after treatment. Tumor volume was manually segmented and calculated by Osirix (http://www.osirixviewer.com). Statistical analysis (paired *t* test) was performed using Prism GraphPad 4 (GraphPad Software). After morphologic T2w imaging, diffusion-weighted MRI (DW-MRI) was performed using a multishot spin echo EPI sequence with a total of 6 diffusion weightings: b0–5 values = 0, 50, 100, 200, 400 and 600 s/mm², slice thickness = 1.4 mm, in plane resolution = $0.62 \times 0.78\,mm^2$, EPI factor = 7, TR/TE = 4907/62 ms, averages = 2. Three center slices in axial orientation, covering each adrenal gland were selected to assess the median apparent diffusion coefficient (ADC) value before and after treatment. Segmented tumors were analyzed by in-house software written in IDL (ITT VIS).

Positron Emission Tomography (PET) imaging

LMI1195 precursor and the method for radiosynthesis of ^{18}F-LMI1195 were provided by Lantheus Medical Imaging (N. Billerica, MA, USA) as previously described (Gaertner *et al.* 2013). The radiochemical purity of ^{18}F-LMI1195 was ≥98% and the specific activity was >600 GBq/μmol. PET was performed using a small animal PET scanner (Inveon Micro PET/CT, Siemens Preclinical

http://erc.endocrinology-journals.org
DOI: 10.1530/ERC-16-0324

Published by Bioscientifica Ltd.

Solutions). Animals were anesthetized by 2% isoflurane inhalation. Animals were injected with 21.4 ± 4.2 MBq ^{18}F-LMI1195 via the tail vein. Static PET scans were started 45 min after tracer injection, and emission time was 15 min. PET data was reconstructed using OSEM 2D, images were corrected for decay, randoms and dead time. Attenuation and scatter correction was not performed. PET images were analyzed using a dedicated workstation (Inveon Research Workplace, version 4.0, Siemens Preclinical Solutions). Quantitative analysis was performed by placing 3D spherical VOIs (volume of interest) around the hottest voxel of the adrenals (15 mm). Standardized uptake values (SUVs) were calculated by SUV = (measured activity (Bq/mL)) × (body weight (g)) ÷ (injected activity (Bq)). Digital sphere phantoms with different volumes were generated to measure recovery coefficients using a combined SimSET (Simulation System for Emission Tomography) and GATE (Geant4 Application for Tomography Emission) Monte-Carlo simulation method. PET sinograms were generated using the geometry of the scintillators and the detector circuitry of the Siemens Inveon scanner 15 (Siemens Healthcare).

Euthanasia and necropsy

Immediately after PET imaging, animals were killed during isoflurane inhalation anesthesia by i.v. injection of sodium pentobarbital 100 mg/kg body weight (Narcoren, Merial GmbH, Hallbergmoos, Germany) and subjected to complete necropsy. Total body and organ weights were measured for each animal.

Statistical analysis

Results of the cell assays or of imaging scans are shown as the mean of values obtained in independent experiments ± S.E.M. A paired two-tailed Student's t test was used to detect the significance between two series of data, and $P < 0.05$ was considered statistically significant.

Results

PI3K/mTOR inhibition shows dose-dependent effects on cell proliferation, cell death and angiogenesis in a model of endogenous PCCs *in vivo*

We previously reported that treatment of primary cultures of MENX-associated PCC cells with the dual PI3K/mTOR inhibitor BEZ235 decreases their proliferation and promotes apoptosis (Lee *et al.* 2012). Similarly, treatment of MPC mouse pheochromocytoma cells with BEZ235 was found to reduce their proliferation (Nölting *et al.* 2012). We extended these studies by showing that BEZ235 also suppresses the ability of MPC cells to migrate and invade (Supplementary Fig. 1, see section on supplementary data given at the end of this article). To characterize the response of PCCs to a blockade of PI3K and mTOR signaling *in vivo*, we treated MENX-affected rats with two different doses of the drug, specifically 20 mg/kg or 30 mg/kg or with PEG vehicle (placebo) by oral gavage for 2 weeks and performed detailed *ex vivo* analyses. We observed a strong dose-dependent reduction of P-S6, a downstream target of PI3K/mTOR pathway, in the rat tumors after treatment with both 20 mg/kg and 30 mg/kg BEZ235 but not after placebo administration (Fig. 1A, B and Supplementary Fig. 2). Concomitantly, there was a significant reduction in cell proliferation (Ki67 and NuSAP staining) and in the levels of the angiogenic factor VEGFA in the PCCs of BEZ235-treated but not of placebo-treated rats (Fig. 1A, B and Supplementary Fig. 2). We also observed a decrease in CD31 expression, a marker of endothelial cells, but it was modest (Fig. 1B and Supplementary Fig. 2). Immunostaining using antibodies against Annexin V and activated caspase-3, both markers of apoptotic cells, showed increased signal after treatment, thereby confirming that BEZ235 induces cells death in PCC (Fig. 1A, B and Supplementary Fig. 2). Altogether, these results demonstrate that PI3K/mTOR inhibition has a dose-dependent cytostatic and cytotoxic effects on PCC.

We then wondered whether therapy response might be monitored non-invasively in rats by functional imaging. Having observed a cytotoxic effect of the drug, we selected diffusion-weighted magnetic resonance imaging (DW-MRI) with calculated mean apparent diffusion coefficient (ADC) values to assess the changes in tumor cellularity as surrogate marker of response to therapy (Thoeny & Ross 2010). ADC values were obtained for the mutant rats ($n = 5$; 10 adrenal glands) at day 0 (pre-therapy scans), and then 14 days after daily administration of 20 mg/kg BEZ235. Three sagittal center slices were used to calculate a mean ADC for each adrenal gland. As shown in Fig. 1C, we observed significantly increased ADC values after BEZ235 treatment (mean ADC pre-treatment vs mean ADC post-treatment: $P = 0.0208$).

In addition to the DW-MRI, we measured volumetric changes of the adrenal glands before and after treatment with BEZ235 or placebo by conventional T2w MRI. No significant differences in adrenal volumes were seen in both BEZ235-treated and placebo-treated rats (data not shown). Probably a 14-day course of treatment is not long enough to elicit tumor shrinkage to an extent detectable

http://erc.endocrinology-journals.org
DOI: 10.1530/ERC-16-0324

Published by Bioscientifica Ltd.

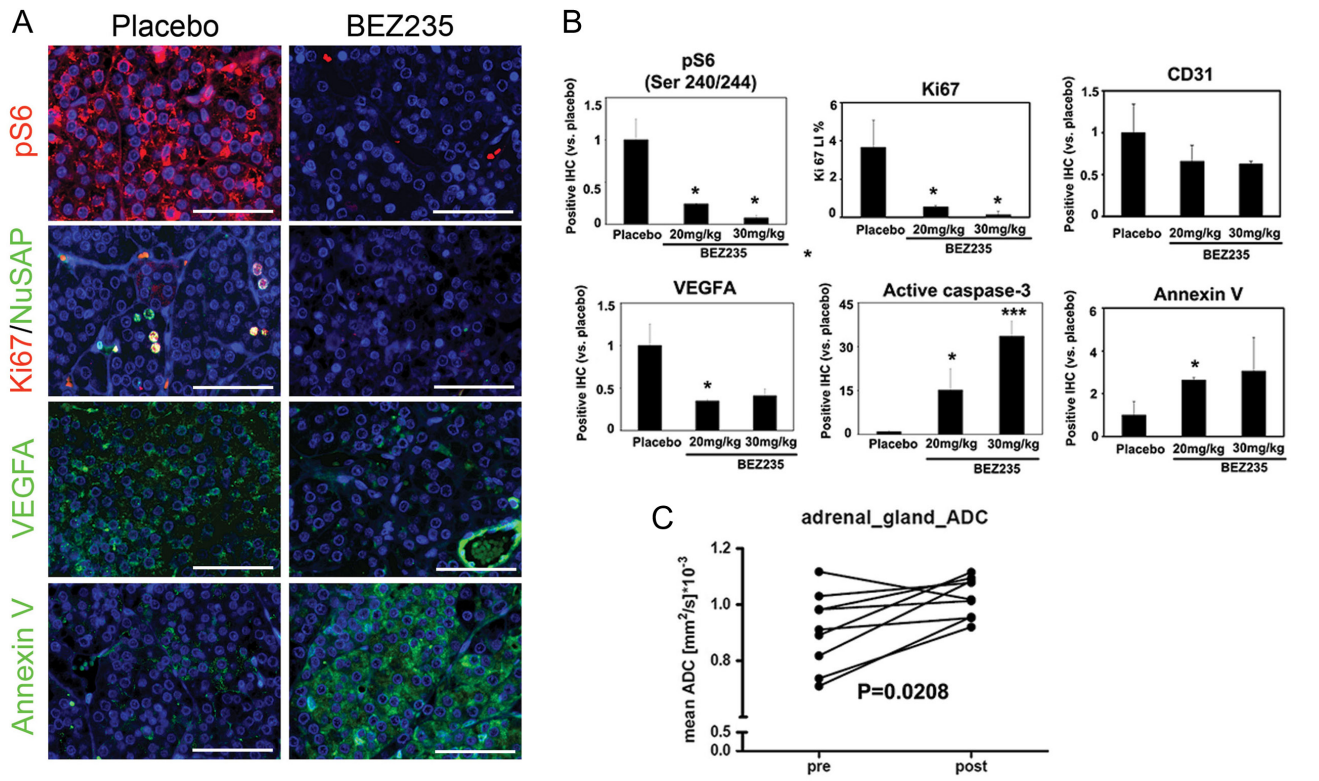

Figure 1
Analysis of PCC tissues from rats treated with placebo or BEZ235. (A) Tumor tissues of MENX-affected rats treated with PEG vehicle (Placebo) or with 30 mg/kg of BEZ235 by oral gavage for 2 weeks. Tissues were collected, fixed in formalin and embedded in paraffin. Immunofluorescent (IF) staining was performed using specific antibodies raised against P-S6 (Ser240/244), Ki67, NuSAP, VEGFA and Annexin V. Cell nuclei were counterstained with DAPI. Scale bars: 50 µm. (B) Quantification of the IF signal of the panels shown in A and in Supplementary Fig. 2 done with ImageJ software for the antibodies against P-S6, CD31, VEGFA, active caspase-3 and Annexin V. For Ki67, the percentage of the positive nuclei was counted in 5× high-power field (HPF) on tissues from 3 different mutant rats for each condition. *$P<0.05$, **$P<0.01$ (C) Apparent diffusion coefficient (ADC) values were obtained by performing DW-MRI before (pre) and after (post) treatment of mutant rats ($n=5$, total adrenal gland number $n=10$) with BEZ235.

by anatomical imaging. Thus, DW-MRI, assessing a functional parameter such as the induction of cell death, might be useful for early response tumor monitoring after PI3K/mTOR inhibition in PCCs before changes in tumor volume take place.

Identification of the genes dysregulated after drug treatment

We then performed gene expression array analyses to identify genes differentially expressed in PCCs obtained from BEZ235-treated (20 and 30 mg/kg) vs placebo-treated rats (Supplementary Fig. 3). Array data were subjected to functional analysis by means of the Ingenuity Pathway Analysis (IPA) software to interpret the biological meaning of the drug treatment. The most differentially expressed genes in the two samples groups (drug- vs placebo-treated tumors) were associated with the categories: cell growth and proliferation, cellular movement, cell death and survival (Supplementary Table 1). Specifically, the functions: proliferation of cells, migration of cells, cell survival and cell viability were associated to a negative *z*-score, indicating that their reduction in the tumor cells of BEZ235-treated rats compared with the placebo-treated rats. Conversely, the functions apoptosis, necrosis and fragmentation of nucleus showed a significant activation in PCC cells upon BEZ235 administration (Supplementary Table 1). These analyses indirectly confirmed the decrease in cell proliferation and increase in apoptosis we have observed in the tissues of the drug-treated rats (Fig. 1A and Supplementary Fig. 2).

Among the genes downregulated after BEZ235 treatment, we found two genes coding for regulatory subunits of the PI3K, namely *Pik3r1* (–1.44 fold), *Pik3r3* (–1.61 fold) and a gene coding for one AKT kinase, *Akt1* (–1.27 fold). This further supports the inhibition of the PI3K pathway by this agent. Genes that usually promote features such as cell proliferation, cell cycle and cell death

Published by Bioscientifica Ltd.

were also downregulated by BEZ235 administration, including *Rrm2* (–2.36)1, *Hdac2* (–1.26)2, *Ccnb1* (–1.59), *Cxcr4* (–1.62) and *Lgals3BP* (–1.68). Rat PCCs were previously shown to have a signature of immature chromaffin cells as they highly express genes involved in sympathoadrenal differentiation (Molatore *et al.* 2010). The expression of some of these developmental genes, namely *NeuroD1* (–1.41), *Phox2a* (–1.31), *Gata2* (–1.60) and *Sema5a* (–1.23) decreased upon drug treatment. Conversely, four genes involved in processes important for chromaffin cell function such as catecholamine secretion or exocytosis (i.e. *Serpine1*, +11.18; *VGF*, +10.42; *SV2c*, +3.37; *Npy*, +1.88) were significantly induced by BEZ235 treatment. Altogether, PI3K/mTOR inhibition induced gene expression changes compatible with reduced proliferation and potential rescue of a more mature phenotype of the chromaffin tumor cells.

The reduction of Slc6a2/NET after BEZ235 treatment in rat tumors and in primary cells

Among the genes dysregulated after BEZ235 treatment, one caught our attention: the *Slc6a2* gene, encoding the norepinephrine transporter (NET). Based on our transcriptome analysis, *Slc6a2* is downregulated by BEZ235 significantly and in a dose-dependent manner. Specifically, in tumor tissues of rats treated with 30 mg/kg of BEZ235, the expression of *Slc6a2* was reduced by –5.60 fold vs placebo and in those of animals treated with 20 mg/kg was repressed by –1.70 fold (Fig. 2A). NET belongs to the family of the monoamine transporters and is involved in the reuptake primarily of norepinephrine but also of dopamine in neural cells and chromaffin cells of the adrenal medulla. NET is also present on the membrane of PCC cells, and it has been heavily exploited for the functional imaging of these tumors, as mentioned earlier.

To verify that indeed BEZ235 treatment decreases the expression of the *Slc6a2* gene, we conducted TaqMan analyses on the same rat tissues used for the expression profiling. The results confirmed that there is a dose-dependent inhibition of *Slc6a2* expression in the PCCs after BEZ235 administration (Fig. 2B). In parallel, we also performed immunohistochemical staining of PCC tissues from rats treated with BEZ235 or with placebo. In agreement with the array and TaqMan results, BEZ2335-treated MENX rats showed a dose-dependent reduction of the NET protein in the tumors (more pronounced in 30 mg/kg-treated than in 20 mg/kg-treated animals) when compared with placebo-treated MENX rats (Fig. 2C).

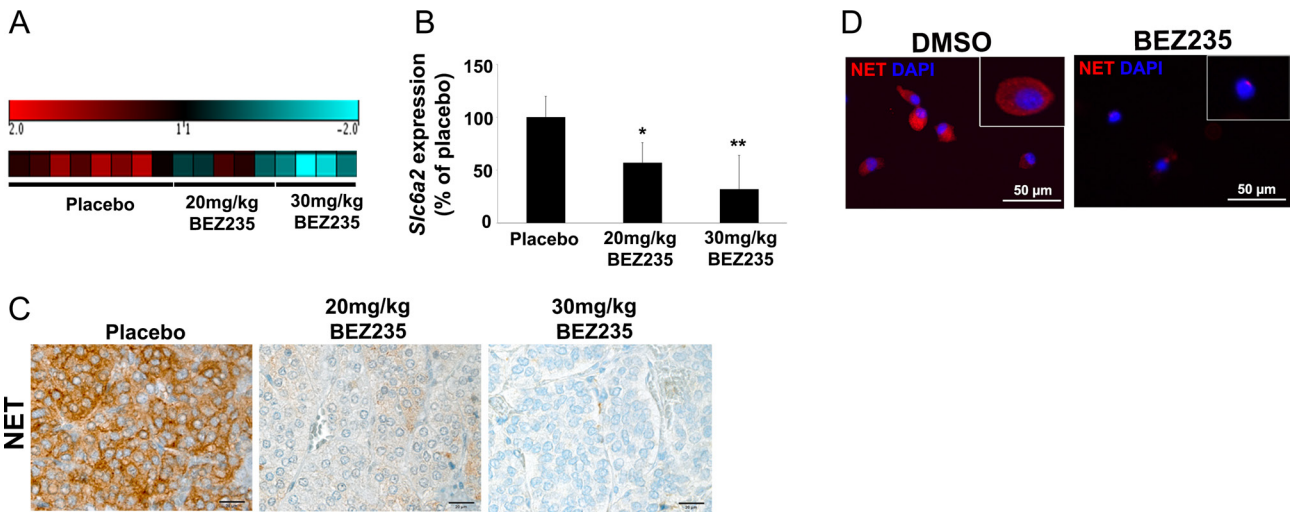

Figure 2
BEZ235 reduces *Slc6a2*/NET expression in rat PCCs *in vivo* and *in vitro*. (A) Heat map showing the relative expression of *Slc6a2* obtained by gene expression profiling of PCCs of rats treated with placebo ($n=8$) or BEZ235 (20 mg/kg, $n=5$; 30 mg/kg, $n=4$) for 14 days. (B) RNA was extracted from the PCCs of the rats used in A. qRT-PCR was performed using TaqMan primer and probe sets specific to rat *Slc6a2*. The relative mRNA expression level of *Slc6a2* was calculated with the $2^{-\Delta\Delta Ct}$ formula and was normalized for input RNA using rat β2-microglobulin gene expression (housekeeping gene). The obtained relative value was normalized against the average expression of placebo-treated tissues arbitrarily set to 100. Data were analyzed independently with six replicates each and are expressed as the mean ± S.E.M. *$P<0.05$. (C) Rat PCCs were collected after 14 days of daily placebo or BEZ235 administration and was analyzed by immunostaining for NET expression. Scale bars: 20 µm. (D) *In vitro* cultures of rat primary PCC cells were treated daily with DMSO vehicle or with BEZ235 (1 µM) for 48 h. Then, they were fixed and immunofluorescent staining was conducted using the anti-NET antibody. Nuclei were counterstained with DAPI. Scale bars: 50 µm.

http://erc.endocrinology-journals.org
DOI: 10.1530/ERC-16-0324

Published by Bioscientifica Ltd.

In silico analysis of previously performed gene expression profiling of MENX-associated adrenomedullary lesions showed that rat PCCs have significantly higher *Slc6a2* expression (+2.52 fold) compared to normal rat adrenal tissue (Molatore *et al*. 2010). Also, isolated rat primary PCC cells in culture express *Slc6a2* at high levels, as demonstrated by immunofluorescence with an anti-NET antibody (Fig. 2D). In agreement with the *ex vivo* data on NET expression in the rat tissues, BEZ235 treatment suppressed NET levels also in rat primary PCC cells *in vitro* (Fig. 2D).

NET expression is downregulated by PI3K/mTOR inhibition in MPC cells

To better study NET expression modulation after dual-PI3K/mTOR inhibition, we extended our analyses to established *in vitro* tumor models. PC12 cells (from a rat PCC), MPC and MTT cells (both from mouse PCC) were analyzed for endogenous *Slc6a2* expression by RT-PCR, and for NET expression by western blotting. Among these cell lines, MPC cells showed the highest level of *Slc6a2*/NET (Fig. 3A). Thus, we assessed whether BEZ235 affects the expression of *Slc6a2*/NET in MPC cells also: exposure to the drug decreased the expression of both the *Slc62a* transcript and the NET protein (Fig. 3B). In parallel, decreased phosphorylation of both Akt (Akt-Ser473) and S6 (S6-S240/244) was seen in the drug-treated vs. vehicle-treated MPC cells indicating that the pathway has been inhibited by the compound, as expected (Fig. 3B). Moreover, PI3K/mTOR inhibition reduced the proliferation of MPC cells (Supplementary Fig. 4).

BEZ235 is a dual-inhibitor that inhibits both catalytic activities of mTOR and of all class I PI3K isoforms by targeting their ATP-binding site. The compound BKM120 inhibits all class I PI3K isoforms, whereas RAD001 specifically inhibits the activity of mTOR. To investigate the specificity of the regulation of *Slc6a2*/NET expression by inhibitors of the PI3K pathway, we incubated MPC cells for 48 h with BKM120, BEZ235 or RAD001 as single agents or with BKM120 in combination with RAD001. As shown in Fig. 3C, BKM120 and RAD001 alone only slightly decreased *Slc6a2* gene expression when compared with BEZ235. In contrast, the combination treatment of BKM120 with RAD001 successfully reduced the *Slc6a2* gene (Fig. 3C). In agreement with the mRNA data, single inhibition by BKM120 or RAD001 completely failed to reduce the NET protein (Fig. 3D), whereas the combination treatment caused a dramatic reduction of the NET protein, similarly to BEZ235 treatment (Fig. 3D). Taken together, these results suggest that the combined inhibition of both PI3K and mTOR signaling is required for an effective reduction of *Slc6a2*/NET expression in PCC cells.

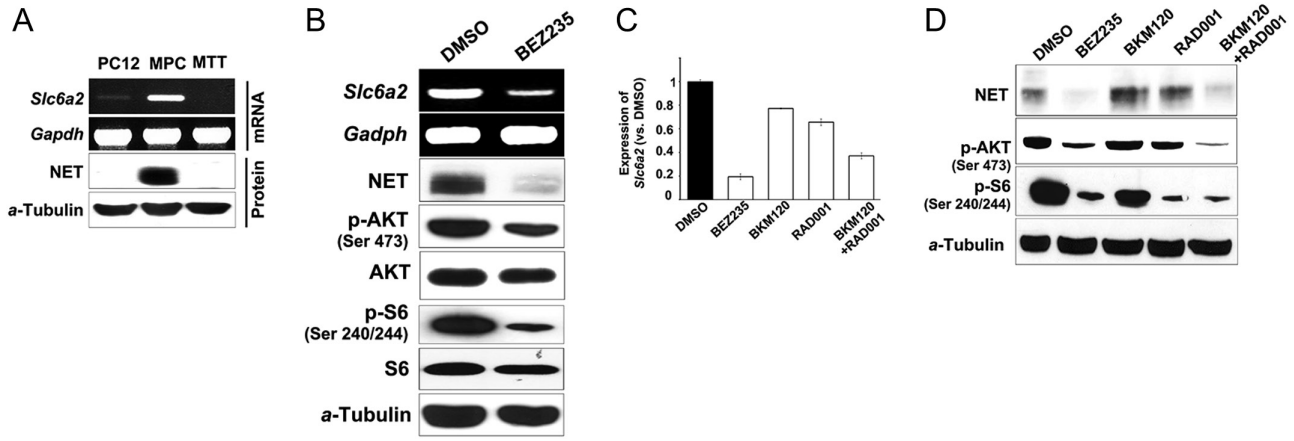

Figure 3
The expression of *Slc6a2*/NET in PCC cells. (A) Semi-quantitative RT-PCR and western blotting specific to the *Slc6a2* gene/NET protein, respectively, were performed using 3 PCC cell lines (PC12, MPC and MTT). As internal control for the mRNA level we used *Gadph*, whereas for the protein level, we used α-tubulin. (B) MPC cells were incubated with DMSO (vehicle) or with 1 μM BEZ235. RNA and proteins were extracted 48 h later. RT-PCR was performed to monitor *Slc6a2* expression as in A. In parallel, NET, AKT, P-AKT (Ser473), S6 and P-S6 (Ser240/244) expression was monitored by western blotting. (C) MPC cells were incubated with 1 μM BEZ235, 1 μM BKM120, 1 μM RAD001 or with the combination BKM120 and RAD001. Control cells were incubated with DMSO (vehicle). RNA was extracted 48 h later, and TaqMan analysis for the *Slc6a2* gene was performed. Shown is the average of the relative expression values were normalized against the β2-microglobulin housekeeping gene and was calculated with the $2^{-\Delta\Delta Ct}$ formula. The obtained relative value was normalized against the average expression of DMSO-treated cells arbitrarily set to 1. Data were analyzed independently with three replicates each and are expressed as the mean ± S.E.M. $^{*}P<0.05$. (D) From samples parallel to C, proteins were extracted after drug treatment, and the expression of NET, P-AKT (Ser473) and P-S6 (Ser240/244) was monitored by western blotting.

http://erc.endocrinology-journals.org
DOI: 10.1530/ERC-16-0324

Published by Bioscientifica Ltd.

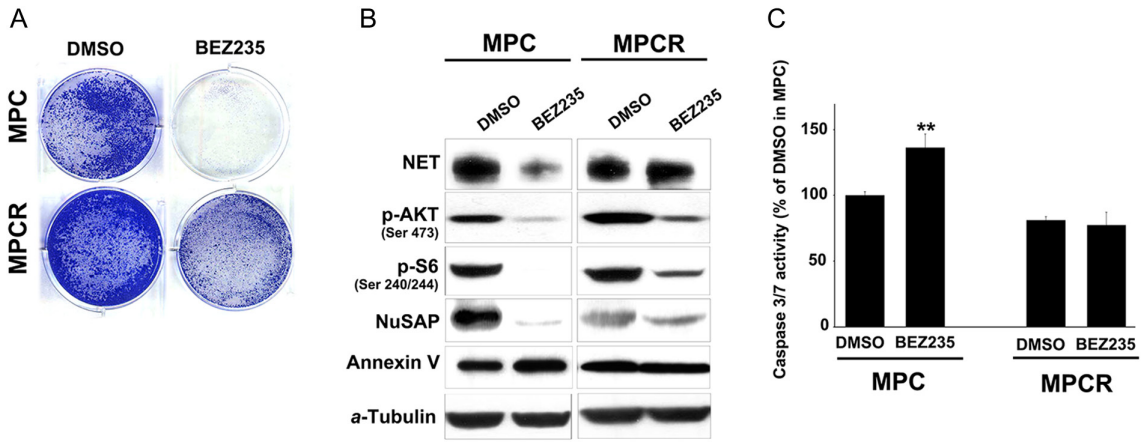

Figure 4
The expression of NET in MPC and MPCR cells after BEZ235 treatment. (A) Colony formation assay of MPC and MPCR cells treated with DMSO (vehicle) or with 1 μM BEZ235 for 2 weeks. Cells were then fixed and stained with crystal violet. Representative plates are shown. (B) MPC and MPCR cells were incubated with DMSO (vehicle) or with 1 μM BEZ235 for 48 h. Proteins were extracted and the expression of NET, p-AKT (Ser473), p-S6 (Ser240/244), NuSAP, Annexin 5 and α-tubulin was detected by western blotting. (C) MPC and MPCR cells were treated as in B and then were monitored for caspase-3/7 activity. Shown is the average of the relative activity normalized against the DMSO-treated cells arbitrarily set to 100. Data were analyzed independently with six replicates each and were expressed as the mean ± S.E.M. $^{**}P < 0.01$.

MPC cells resistant to BEZ235 do not suppress NET expression

We next decided to assess whether NET expression might be predictive of the response of PCC cells to dual-PI3K/mTOR inhibition. To this aim, we generated a BEZ235-resistant, MPC-derived cell line (named MPCR) by treating the cells with the drug over a period of 8 weeks. To confirm the resistance of MPCR cells to PI3K/mTOR inhibition, we performed colony formation assays using MPC and MPCR cells in the presence or absence of BEZ235. As expected, MPCR cells formed colonies in the presence of the drug, whereas the parental MPC cells did not (Fig. 4A). Similarly, downstream targets of the PI3K/mTOR pathway (P-AKT and P-S6) as well as a proliferation marker (NuSAP) were not much affected by the drug in MPCR cells, whereas they were strongly reduced in the drug-sensitive MPC cells (Fig. 4B). Having assessed that MPCR cells do not respond to PI3K/mTOR inhibition (we see no inactivation of the downstream targets nor a reduction of markers of proliferation), we then compared the expression of the NET protein between MPC and MPCR cells after BEZ235 treatment. We found that MPCR

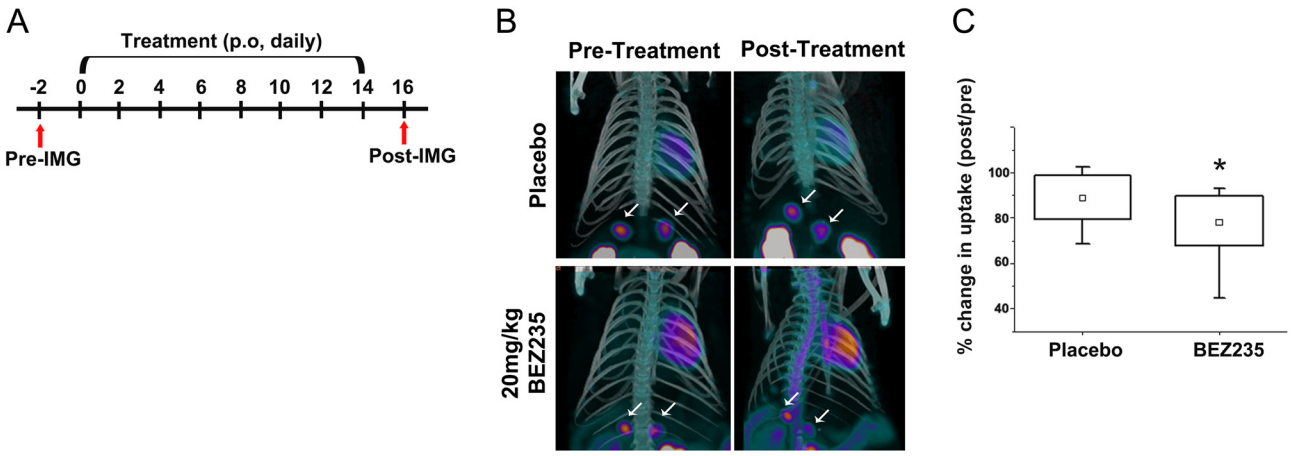

Figure 5
Functional imaging with ^{18}F-LMI1195 to monitor the response of rat PCCs to BEZ235 *in vivo*. (A) Scheme of the treatment course. PET imaging (IMG) was performed before (pre) and after (post) treatment with placebo (PEG) or BEZ235 for 14 days. (B) Representative images of the PET scans obtained for the same mutant rats before and after treatment with placebo or BEZ235. Arrows indicate the adrenal glands. (C) Quantitative analysis of PET images of ^{18}F-LMI1195 in placebo-treated ($n = 5$; 10 adrenals) and BEZ235-treated MENX rats ($n = 8$; 16 adrenals).

Published by Bioscientifica Ltd.

cells fail to reduce the NET expression after drug treatment (Fig. 4B). In addition, we measured apoptosis in both cell lines 48 h after BEZ235 treatment. MPCR cells show no increase in apoptosis, whereas a 30% increase in apoptosis was seen in the parental MPC cells (Fig. 4C).

Altogether, these results suggest that the reduction of NET expression is associated to the response of PCC to PI3K/mTOR inhibition.

Reduced uptake of ^{18}F-LMI11195 by PCCs after BEZ235 treatment *in vivo*

Surrogate markers of therapy response that can be easily and reliably monitored during treatment are extremely useful to help stratify patients and make decisions about continuation or discontinuation of treatment. In a previous study, we have shown that rat PCCs can be visualized non-invasively *in vivo* by PET imaging using tracers targeting the NET system, including ^{68}Ga-HED (25) and ^{18}F-LMI1195 (Gaertner *et al.* 2013), a novel norepinephrine analogue. To verify whether the downregulation of NET induced by the inhibition of PI3K/mTOR signaling might also affect the uptake of NET-targeting tracers *in vivo*, we performed PET imaging of MENX rats using ^{18}F-LMI1195. Specifically, ^{18}F-LMI1195 imaging was obtained for a group of 8 rats before treatment (pre-therapy) and then again 14 days after treatment with 20 mg/kg BEZ235 (post-therapy) (Fig. 5A). The uptake of ^{18}F-LMI1195 by the adrenal glands of MENX-affected rats decreased after drug administration (–27% after vs before treatment; $P=0.039$), suggesting reduced functional NET expression (Fig. 5B and C). Altogether, these results suggest that molecular imaging targeting the NET system can be employed to monitor the response of PCC to PI3K/mTOR inhibition therapy.

Discussion

In our study, we assessed the efficacy of PI3K/mTOR inhibition for the therapy of PCC in an *in vivo* model of endogenous tumors (e.g. MENX rats), which recapitulate the important features of human PCCs. We here demonstrate that treatment with the dual-PI3K/mTOR inhibitor BEZ235 displays both cytostatic and cytotoxic activities against PCC. Transcriptome analysis of the rat tumor tissues discovered genes regulated by BEZ235 and identified NET as a novel downstream target of the PI3K pathway in PCC cells.

We selected to target the PI3K/AKT/mTOR signaling cascade because, similar to a great variety of other tumors, both rat and human PCCs show hyperactivation of this pathway. Indeed, a significant increase in the P-AKT/total AKT ratio was observed in human PCCs, which was related neither to loss of heterozygosity of *PTEN* nor to reduced PTEN protein expression (Fassnacht *et al.* 2005). Moreover, it has been reported that S6K1, a downstream target of mTOR, plays a pivotal role in the regulation of mouse adrenal medullary cells proliferation, and it is expressed at high level in 25% of human PCCs (Nardella *et al.* 2011). Thus, targeting the PI3K signaling pathway with a dual PI3K/mTOR inhibitor seemed worth exploring as a novel therapeutic strategy for PCC. Indeed, these compounds can prevent the development of drug resistance, which is usually associated with drugs targeting mTOR alone (rapalogs). Interestingly, previous studies demonstrated a strong inhibition of the proliferation of PCC cell lines *in vitro* by BEZ235 (Nölting *et al.* 2012), and we have reported that BEZ235 potently reduces the proliferation of rat primary PCC cells *in vitro* (Lee *et al.* 2012), thereby further supporting the promising effects of this compound. Here, we show that the *in vivo* treatment of rat PCCs with BEZ235 suppresses the expression of proteins associated with cell proliferation, such as Ki67 and NuSAP, a protein shown to correlate with cell division in human neuroendocrine tumors (Lee *et al.* 2013). In parallel, drug treatment downregulated VEGFA, the best characterized angiogenic marker, and upregulated markers of apoptosis such as active caspase-3 and Annexin V. A cytotoxic effect of BEZ235 has been reported in various human cancers (Chen *et al.* 2014, Bendell *et al.* 2015, Fazio *et al.* 2016). We previously reported that BEZ235 induces the death of pituitary adenoma cells and that this effect is partially mediated by an active apoptotic process (Lee *et al.* 2015). Consistent with the induction of apoptosis in the PCC tissues of BEZ235-treated MENX rats, also the incubation of MPC cells with this drug promoted caspase 3/7 activity *in vitro*. Further support to a pro-apoptotic role of BEZ235 in PCC comes from the transcriptome profiling of treated vs untreated rat tissues, showing that among the deregulated genes, many belong to the cell death category. Nölting and coworkers (2012) observed no induction of apoptosis upon incubation of the aggressive PCC cell line MTT with BEZ235. In that study, MPC cells after BEZ235 treatment were not analyzed for the induction of apoptosis. Based on our results, MTT cells, in contrast to MPC cells and to rat primary PCC cells, do not express significant levels of NET. Thus, the pro-apoptotic activity of dual PI3K/mTOR inhibition in adrenal medullary tumor cells may require NET expression.

http://erc.endocrinology-journals.org
DOI: 10.1530/ERC-16-0324

Published by Bioscientifica Ltd.

Based on RECIST criteria (Eisenhauer *et al.* 2009), it typically takes several months to evaluate therapy response of many solid tumors when using morphological imaging methods such as CT or MRI exclusively. Thus, early markers able to predict the response to PI3K/mTOR inhibitors would help to better leverage the clinical application of these drugs. The relevance of predictive markers of response to mTOR inhibition in neuroendocrine tumors has recently been reviewed by Zatelli and coworkers (2016). In this context, surrogate markers of therapy response that could be assessed by functional imaging modalities could help to quickly identify non-responders, thereby minimizing potential side effects (and costs) of an ineffective therapy. In our study, we showed that non-invasive DW-MRI is a useful imaging modality for the early therapy response monitoring of PCCs treated with a PI3K/mTOR inhibitor. DW imaging can characterize tumor physiology and morphology, as well as provide information about cellular consistency, which associates with lower (=less cellularity) or higher (=higher cellularity) ADC values. A significant increase in ADC values was observed in rat adrenals after only 2 weeks of BEZ235 administration, which mirrored the enhanced cell death observed in tumor tissues *ex vivo*. Interestingly, changes in ADC values after drug treatment preceded changes in adrenal gland volume, as measured by conventional anatomical MRI.

In addition to establishing whether BEZ235 has antitumor effects in PCC, we were also interested in identifying novel downstream effectors of PI3K/mTOR inhibition. To this aim, we conducted genome-wide transcriptome profiling of PCCs from rats treated with BEZ235 (at 2 different doses) or with placebo. The genes differentially expressed between the treated and untreated tumors are enriched in transcripts involved in tumor-associated processes such as cell migration, proliferation, growth and cell death. Specifically, the direction of gene dysregulation (*z* score) supports the hypothesis that cell migration, proliferation, growth, angiogenesis and protein translation are reduced upon drug treatment, whereas cell death, necrosis and apoptosis are promoted by BEZ235. The drug also reduces the expression of genes responsible for the progenitor-like signature of rat PCCs (Molatore *et al.* 2010).

Interestingly, after a blockade of PI3K/mTOR signaling, we observed a reduction in the expression of the *Slc6a2* gene and of the encoded NET protein both *in vitro* (primary rat PCC cells) and *in vivo* (MENX rats). This reduction was not limited to MENX-associated PCCs, but also extended to the MPC cell line. *In vitro,* a more pronounced downregulation of NET expression was obtained after the inhibition of both PI3K and mTOR signaling when compared to the inhibition of the single molecules. To assess whether the reduction of NET expression could predict the ability of PCC cells to respond to BEZ235, we generated a MPC-derived clonal cell population resistant to the drug (called MPCR). These resistant cells showed, after treatment, an extremely modest reduction in the amount of activated downstream targets of the PI3K/mTOR pathway (P-AKT, P-S6) compared to the parental MPC cells. Moreover, treatment of MPCR cells with BEZ235 did not induce a pro-apoptotic molecule (Annexin V), nor it induced caspase 3/7 activity, indicating that these cells are no longer affected by the drug. In parallel, we could observe no reduction of NET expression in MPCR cells after treatment with BEZ235. These studies support our hypothesis that the modulation of *Slc6a2*/NET expression in PCC cells upon dual PI3K/mTOR inhibition is required for the response to the drug.

Norepinephrine uptake is regulated by a variety of stimuli, including PI3K-dependent signaling. It has been reported that a member of the rab3 GTPases, rab3B, not only modulates catecholamine secretion but also promotes the rate and accumulation of exogenous norepinephrine in PC12 cells through direct binding and stimulation of PI3K activity (Francis *et al.* 2002). Moreover, it has been shown that basal norepinephrine transport in human SK-N-SH neuroblastoma cells (extensively used as a model of noradrenergic cells) is regulated by PI3K-dependent pathways and can be reduced by the inhibitors of tyrosine kinases and PI3K (Apparsundaram *et al.* 2001). Our findings suggest that the molecular mechanism mediating the above-mentioned effects could be a regulation of *Slc6a2*/NET expression by PI3K signaling, as we observed in rat primary PCC cells and in MPC cells.

In a previous study, we demonstrated that the novel tracer ^{18}F-LMI1195 (a norepinephrine analogue) is rapidly and specifically taken up by rat PCC cells, and it can be used to visualize these tumors as effectively as MIBG (Gaertner *et al.* 2013). Importantly, the BEZ235-induced decrease in the amount of functional norepinephrine transporters present on the surface of PCC cells could be detected by non-invasive functional imaging *in vivo*. Indeed, the uptake of ^{18}F-LMI1195 by rat adrenal glands was significantly decreased after a 2-week treatment regimen with BEZ235. Therefore, in addition to visualize PCCs, ^{18}F-LMI1195 PET imaging might also represent a useful tool to assess the response of these tumors to

http://erc.endocrinology-journals.org
DOI: 10.1530/ERC-16-0324

Published by Bioscientifica Ltd.

PI3K/mTOR inhibitors. Up to date, there have been a few studies about the functional imaging modalities that could monitor the response of various tumors to PI3K/mTOR inhibition. We have shown that DW-MRI might be useful to assess the early cellular response of PCC (this study) or pituitary adenomas (Lee *et al.* 2015) to BEZ235. Other groups demonstrated that the cellular and vascular response of ovarian cancer xenografts to BEZ235 treatment may be detected by using DW-MRI and dynamic contrast-enhanced (DCE) MRI, respectively (Cebulla *et al.* 2015). The early response of anaplastic large cell lymphoma xenografts to BGT226, another dual PI3K/mTOR inhibitor, could be monitored with both ^{18}F-labeled deoxyglucose (FDG-PET) and 3′-deoxy-3′-^{18}F-fluorothymidine (FLT-PET) (Graf *et al.* 2014). To our knowledge, this is the first study using a cell-type specific tracer, targeting the NET, to monitor the response to PI3K/mTOR inhibition by PET imaging.

In conclusion, our findings establish PI3K/mTOR inhibition as an effective therapeutic option for PCC. NET expression emerges as a putative predictive biomarker of the response of PCC cells to a blockade of PI3K and mTOR signaling, which can be assessed by functional imaging. These preclinical trials performed on an endogenous model of PCC provide the rationale for targeting PI3K/mTOR signaling in patients, especially those with aggressive or malignant tumors currently orphan of effective treatment options.

Supplementary data

This is linked to the online version of the paper at http://dx.doi.org/10.1530/ERC-16-0324.

Declaration of interest

The authors declare that there is no conflict of interest that could be perceived as prejudicing the impartiality of the research reported.

Funding

N S Pellegata is supported by grants SFB824, subproject B08, from the Deutsche Forschungs-gemeinschaft (DFG) and grant #110874 from the Deutsche Krebshilfe.

Acknowledgements

The authors thank Elke Pulz and Anke Bettenbrock for excellent technical assistance, Sybille Reder for help with PET imaging and Novartis for providing us with BEZ235. The authors acknowledge the support of grants from the Helmholtz Portfolio Theme 'Metabolic Dysfunction and Common Disease' and the Helmholtz Alliance 'Imaging and Curing Environmental Metabolic Diseases, ICEMED' (to J B).

References

Apparsundaram S, Sung U, Price RD & Blakely RD 2001 Trafficking-dependent and -independent pathways of neurotransmitter transporter regulation differentially involving p38 mitogen-activated protein kinase revealed in studies of insulin modulation of norepinephrine transport in SK-N-SH cells. *Journal of Pharmacology and Experimental Therapeutics* **299** 666–677.

Averbuch SD, Steakley CS, Young RC, Gelmann EP, Goldstein DS, Stull R & Keiser HR 1988 Malignant pheochromocytoma: effective treatment with a combination of cyclophosphamide, vincristine, and dacarbazine. *Annals of Internal Medicine* **109** 267–273. (doi:10.7326/0003-4819-109-4-267)

Baumann P, Mandl-Weber S, Oduncu F & Schmidmaier R 2009 The novel orally bioavailable inhibitor of phosphoinositol-3-kinase and mammalian target of rapamycin, NVP-BEZ235, inhibits growth and proliferation in multiple myeloma. *Experimental Cell Research* **315** 485–497. (doi:10.1016/j.yexcr.2008.11.007)

Bendell JC, Kurkjian C, Infante JR, Bauer TM, Burris HA 3rd, Greco FA, Shih KC, Thompson DS, Lane CM, Finney LH, *et al.* 2015 A phase 1 study of the sachet formulation of the oral dual PI3K/mTOR inhibitor BEZ235 given twice daily (BID) in patients with advanced solid tumors. *Investigational New Drugs* **33** 463–471. (doi:10.1007/s10637-015-0218-6)

Cantrell DA 2001 Phosphoinositide 3-kinase signaling pathways. *Journal of Cell Science* **114** 1439–1445.

Cao P, Maira SM, Garcia-Echeverria C & Hedley DW 2009 Activity of a novel, dual PI3-kinase/mTor inhibitor NVP-BEZ235 against primary human pancreatic cancers grown as orthotopic xenografts. *British Journal of Cancer* **100** 1267–1276. (doi:10.1038/sj.bjc.6604995)

Cebulla J, Huuse EM, Pettersen K, van der Veen A, Kim E, Andersen S, Prestvik WS, Bofin AM, Pathak AP, Bjorkoy G, *et al.* 2015 MRI reveals the in vivo cellular and vascular response to BEZ235 in ovarian cancer xenografts with different PI3-kinase pathway activity. *British Journal of Cancer* **112** 504–513. (doi:10.1038/bjc.2014.628)

Chen J, Zhao KN, Li R, Shao R & Chen C 2014 Activation of PI3K/Akt/mTOR pathway and dual inhibitors of PI3K and mTOR in endometrial cancer. *Current Medicinal Chemistry* **21** 3070–3080. (doi:10.2174/0929867321666140414095605)

Druce MR, Kaltsas GA, Fraenkel M, Gross DJ & Grossman AB 2009 Novel and evolving therapies in the treatment of malignant phaeochromocytoma: experience with the mTOR inhibitor everolimus (RAD001). *Hormone and Metabolic Research* **41** 697–702. (doi:10.1055/s-0029-1220687)

Eisenhauer EA, Therasse P, Bogaerts J, Schwartz LH, Sargent D, Ford R, Dancey J, Arbuck S, Gwyther S, Mooney M, *et al.* 2009 New response evaluation criteria in solid tumours: revised RECIST guideline (version 1.1). *European Journal of Cancer* **45** 228–247. (doi:10.1016/j.ejca.2008.10.026)

Eisenhofer G, Bornstein SR, Brouwers FM, Cheung NK, Dahia PL, de Krijger RR, Giordano TJ, Greene LA, Goldstein DS, Lehnert H, *et al.* 2004 Malignant pheochromocytoma: current status and initiatives for future progress. *Endocrine-Related Cancer* **11** 423–436. (doi:10.1677/erc.1.00829)

Eisenhofer G, Pacak K, Huynh TT, Qin N, Bratslavsky G, Linehan WM, Mannelli M, Friberg P, Grebe SK, Timmers HJ, *et al.* 2011 Catecholamine metabolomic and secretory phenotypes in phaeochromocytoma. *Endocrine-Related Cancer* **18** 97–111. (doi:10.1677/ERC-10-0211)

Fassnacht M, Weismann D, Ebert S, Adam P, Zink M, Beuschlein F, Hahner S & Allolio B 2005 AKT is highly phosphorylated in pheochromocytomas but not in benign adrenocortical tumors. *Journal of Clinical Endocrinology and Metabolism* **90** 4366–4370. (doi:10.1210/jc.2004-2198)

Fazio N, Buzzoni R, Baudin E, Antonuzzo L, Hubner RA, Lahner H, DE Herder WW, Raderer M, Teule A, Capdevila J, *et al.* 2016 A phase II

Published by Bioscientifica Ltd.

study of BEZ235 in patients with everolimus-resistant, advanced pancreatic neuroendocrine tumours. *Anticancer Research* **36** 713–719.
Francis SC, Sunshine C & Kirk KL 2002 Coordinate regulation of catecholamine uptake by rab3 and phosphoinositide 3-kinase. *Journal of Biological Chemistry* **277** 7816–7823. (doi:10.1074/jbc.M109743200)
Gaertner FC, Wiedemann T, Yousefi BH, Lee M, Repokis I, Higuchi T, Nekolla SG, Yu M, Robinson S, Schwaiger M, *et al.* 2013 Preclinical evaluation of 18F-LMI1195 for in vivo imaging of pheochromocytoma in the MENX tumor model. *Journal of Nuclear Medicine* **54** 2111–2117. (doi:10.2967/jnumed.113.119966)
Ghayee HK, Giubellino A, Click A, Kapur P, Christie A, Xie XJ, Martucci V, Shay JW, Souza RF & Pacak K 2013 Phospho-mTOR is not upregulated in metastatic SDHB paragangliomas. *European Journal of Clinical Investigation* **43** 970–977. (doi:10.1111/eci.12127)
Graf N, Li Z, Herrmann K, Weh D, Aichler M, Slawska J, Walch A, Peschel C, Schwaiger M, Buck AK, *et al.* 2014 Positron emission tomographic monitoring of dual phosphatidylinositol-3-kinase and mTOR inhibition in anaplastic large cell lymphoma. *OncoTargets and Therapy* **7** 789–798. (doi:10.2147/OTT.S59314)
Hennessy BT, Smith DL, Ram PT, Lu Y & Mills GB 2005 Exploiting the PI3K/AKT pathway for cancer drug discovery. *Nature Reviews Drug Discovery* **4** 988–1004. (doi:10.1038/nrd1902)
Hosoi H, Dilling MB, Liu LN, Danks MK, Shikata T, Sekulic A, Abraham RT, Lawrence JC Jr & Houghton PJ 1998 Studies on the mechanism of resistance to rapamycin in human cancer cells. *Molecular Pharmacology* **54** 815–824.
Huang H, Abraham J, Hung E, Averbuch S, Merino M, Steinberg SM, Pacak K & Fojo T 2008 Treatment of malignant pheochromocytoma/paraganglioma with cyclophosphamide, vincristine, and dacarbazine: recommendation from a 22-year follow-up of 18 patients. *Cancer* **113** 2020–2028. (doi:10.1002/cncr.23812)
Joshua AM, Ezzat S, Asa SL, Evans A, Broom R, Freeman M & Knox JJ 2009 Rationale and evidence for sunitinib in the treatment of malignant paraganglioma/pheochromocytoma. *Journal of Clinical Endocrinology and Metabolism* **94** 5–9. (doi:10.1210/jc.2008-1836)
Lee M, Waser B, Reubi JC & Pellegata NS 2012 Secretin receptor promotes the proliferation of endocrine tumor cells via the PI3K/AKT pathway. *Molecular Endocrinology* **26** 1394–1405. (doi:10.1210/me.2012-1055)
Lee M, Marinoni I, Irmler M, Psaras T, Honegger JB, Beschorner R, Anastasov N, Beckers J, Theodoropoulou M, Roncaroli F, *et al.* 2013 Transcriptome analysis of MENX-associated rat pituitary adenomas identifies novel molecular mechanisms involved in the pathogenesis of human pituitary gonadotroph adenomas. *Acta Neuropathologica* **126** 137–150. (doi:10.1007/s00401-013-1132-7)
Lee M, Wiedemann T, Gross C, Leinhauser I, Roncaroli F, Braren R & Pellegata NS 2015 Targeting PI3K/mTOR signaling displays potent antitumor efficacy against nonfunctioning pituitary adenomas. *Clinical Cancer Research* **21** 3204–3215. (doi:10.1158/1078-0432.CCR-15-0288)
Leinhäuser I, Richter A, Lee M, Hofig I, Anastasov N, Fend F, Ercolino T, Mannelli M, Gimenez-Roqueplo AP, Robledo M, *et al.* 2015 Oncogenic features of the bone morphogenic protein 7 (BMP7) in pheochromocytoma. *Oncotarget* **6** 39111–39126.
Lenders JW, Eisenhofer G, Mannelli M & Pacak K 2005 Phaeochromocytoma. *Lancet* **366** 665–675. (doi:10.1016/S0140-6736(05)67139-5)
Loh KC, Fitzgerald PA, Matthay KK, Yeo PP & Price DC 1997 The treatment of malignant pheochromocytoma with iodine-131 metaiodobenzylguanidine (131I-MIBG): a comprehensive review of 116 reported patients. *Journal of Endocrinological Investigation* **20** 648–658. (doi:10.1007/BF03348026)
Maira SM, Stauffer F, Brueggen J, Furet P, Schnell C, Fritsch C, Brachmann S, Chene P, De Pover A, Schoemaker K, *et al.* 2008 Identification and characterization of NVP-BEZ235, a new orally available dual phosphatidylinositol 3-kinase/mammalian target of rapamycin inhibitor with potent in vivo antitumor activity. *Molecular Cancer Therapeutics* **7** 1851–1863. (doi:10.1158/1535-7163.MCT-08-0017)
Miederer M, Molatore S, Marinoni I, Perren A, Spitzweg C, Reder S, Wester HJ, Buck AK, Schwaiger M & Pellegata NS 2011 Functional Imaging of Pheochromocytoma with Ga-DOTATOC and C-HED in a genetically defined rat model of multiple endocrine neoplasia. *International Journal of Molecular Imaging* **2011** 175352. (doi:10.1155/2011/175352)
Molatore S, Liyanarachchi S, Irmler M, Perren A, Mannelli M, Ercolino T, Beuschlein F, Jarzab B, Wloch J, Ziaja J, *et al.* 2010 Pheochromocytoma in rats with multiple endocrine neoplasia (MENX) shares gene expression patterns with human pheochromocytoma. *PNAS* **107** 18493–18498. (doi:10.1073/pnas.1003956107)
Moraitis AG, Martucci VL & Pacak K 2014 Genetics, diagnosis, and management of medullary thyroid carcinoma and pheochromocytoma/paraganglioma. *Endocrine Practice* **20** 176–187. (doi:10.4158/EP13268.RA)
Nardella C, Lunardi A, Fedele G, Clohessy JG, Alimonti A, Kozma SC, Thomas G, Loda M & Pandolfi PP 2011 Differential expression of S6K2 dictates tissue-specific requirement for S6K1 in mediating aberrant mTORC1 signaling and tumorigenesis. *Cancer Research* **71** 3669–3675. (doi:10.1158/0008-5472.CAN-10-3962)
Nölting S, Garcia E, Alusi G, Giubellino A, Pacak K, Korbonits M & Grossman AB 2012 Combined blockade of signalling pathways shows marked anti-tumour potential in phaeochromocytoma cell lines. *Journal of Molecular Endocrinology* **49** 79–96. (doi:10.1530/jme-12-0028)
Oh DY, Kim TW, Park YS, Shin SJ, Shin SH, Song EK, Lee HJ, Lee KW & Bang YJ 2012 Phase 2 study of everolimus monotherapy in patients with nonfunctioning neuroendocrine tumors or pheochromocytomas/paragangliomas. *Cancer* **118** 6162–6170. (doi:10.1002/cncr.27675)
Pellegata NS, Quintanilla-Martinez L, Siggelkow H, Samson E, Bink K, Hofler H, Fend F, Graw J & Atkinson MJ 2006 Germ-line mutations in p27Kip1 cause a multiple endocrine neoplasia syndrome in rats and humans. *PNAS* **103** 15558–15563. (doi:10.1073/pnas.0603877103)
Porta C, Paglino C & Mosca A 2014 Targeting PI3K/Akt/mTOR signaling in cancer. *Frontiers in Oncology* **4** 64. (doi:10.3389/fonc.2014.00064)
Rainer J, Sanchez-Cabo F, Stocker G, Sturn A & Trajanoski Z 2006 CARMAweb: comprehensive R- and bioconductor-based web service for microarray data analysis. *Nucleic Acids Research* **34** W498–W503. (doi:10.1093/nar/gkl038)
Saeed AI, Sharov V, White J, Li J, Liang W, Bhagabati N, Braisted J, Klapa M, Currier T, Thiagarajan M, *et al.* 2003 TM4: a free, open-source system for microarray data management and analysis. *Biotechniques* **34** 374–378.
Schnell CR, Stauffer F, Allegrini PR, O'Reilly T, McSheehy PM, Dartois C, Stumm M, Cozens R, Littlewood-Evans A, Garcia-Echeverria C, *et al.* 2008 Effects of the dual phosphatidylinositol 3-kinase/mammalian target of rapamycin inhibitor NVP-BEZ235 on the tumor vasculature: implications for clinical imaging. *Cancer Research* **68** 6598–6607. (doi:10.1158/0008-5472.CAN-08-1044)
Serra V, Markman B, Scaltriti M, Eichhorn PJ, Valero V, Guzman M, Botero ML, Llonch E, Atzori F, Di Cosimo S, *et al.* 2008 NVP-BEZ235, a dual PI3K/mTOR inhibitor, prevents PI3K signaling and inhibits the growth of cancer cells with activating PI3K mutations. *Cancer Research* **68** 8022–8030. (doi:10.1158/0008-5472.CAN-08-1385)
Shyla A, Holzlwimmer G, Calzada-Wack J, Bink K, Tischenko O, Guilly MN, Chevillard S, Samson E, Graw J, Atkinson MJ, *et al.* 2010 Allelic loss of chromosomes 8 and 19 in MENX-associated rat

Published by Bioscientifica Ltd.

pheochromocytoma. *International Journal of Cancer* **126** 2362–2372. (doi:10.1002/ijc.24925)

Thoeny HC & Ross BD 2010 Predicting and monitoring cancer treatment response with diffusion-weighted MRI. *Journal of Magnetic Resonance Imaging* **32** 2–16. (doi:10.1002/jmri.22167)

Wiedemann T, Peitzsch M, Qin N, Neff F, Ehrhart-Bornstein M, Eisenhofer G & Pellegata NS 2016 Morphology, biochemistry and pathophysiology of MENX-related pheochromocytoma recapitulate the clinical features. *Endocrinology* **157** 3157–3166. (doi:10.1210/en.2016-1108)

Zatelli MC, Fanciulli G, Malandrino P, Ramundo V, Faggiano A, Colao A & NIKE Group 2016 Predictive factors of response to mTOR inhibitors in neuroendocrine tumours. *Endocrine-Related Cancer* **23** R173–R183. (doi:10.1530/ERC-15-0413)

Received in final form 19 October 2016
Accepted 3 November 2016
Accepted Preprint published online 3 November 2016

Published by Bioscientifica Ltd.